# Hybrid Reduced Order Model For $N_2$-$N_2$ Interactions For Application To Dissociation And Energy Transfer Processes

Robyn L. Macdonald[1], Richard L. Jaffe[2] and Marco Panesi[1]

[1]*University of Illinois at Urbana-Champaign, Urbana, IL, 61801*
[2]*NASA Ames Research Center, Moffett Field, CA, 94035*

**Abstract.** This work presents a general framework for model reduction of non-equilibrium energy transfer and dissociation processes. The multi-group maximum-entropy method is coupled with the quasi-classical trajectory method to directly construct a reduced order model for chemical non-equilibrium. Kinetic data is calculated by applying detailed balance at a microscopic level, overcoming the limitation of calculating recombination kinetic data. This approach enables the construction of a reduced order model for kinetics which bypasses the need to compute state-to-state kinetic data. This physics based reduced order model ensures that an equilibrium distribution is reached given infinite time, while allowing for non-equilibrium distributions during the relaxation and dissociation processes. A proof-of-concept test case demonstrates the applicability of this model by comparison with state-to-state kinetic data for the $N_2(X^1\Sigma_g^+) - N(^4S_u)$ system with excellent agreement.

## INTRODUCTION

Using the quasi-classical trajectory (QCT) method allows for the direct computation of microscopic state-to-state (StS) reaction rate coefficients or cross-sections. This approach in conjunction with the potential energy surface provided by solving the Schrödinger equation has been used to construct a highly accurate StS model for the $N_2(X^1\Sigma_g^+) - N(^4S_u)$ system. [1, 2] This data has enabled StS studies of the non-equilibrium energy transfer and dissociation processes.[3, 4, 5] However, this approach has two main limitations: first it is not practical for application to a multi-dimensional computational fluid dynamics (CFD) or direct simulation Monte Carlo (DSMC) study, and second, extending this approach to interactions between molecules (*e.g.*, diatom-diatom interactions) becomes impossible due to the massive number of collisions which need to be simulated. There has been work to overcome this limitation by using approaches such as applying scaling factors to rates for a subset of the full system, [6] or using the maximum entropy formulation described by Levine and Bernstein[7] to retrieve state-specific reaction rates. [8] However, because these approaches strive to retrieve the StS kinetic mechanism, the problem of using the data remains.

The limitations of the StS approach has motivated the development of reduced order models which aim to capture the same physics as StS models at a fraction of the cost. The multi-group maximum entropy coarse-grain model (MGME-CGM), first proposed by Panesi *et al* [9] and generalized by Liu *et al* [10], aims to accomplish this by grouping energy states together, reducing the number of governing equations. The distribution of states can be retrieved using a functional form derived by maximizing the entropy of the system. One of the advantages of this approach is that it encompasses both the StS and multi-temperature models, with each of these being a particular case of the MGME-CGM. For example, a vibrational StS model is derived by assuming that each group contains a single vibrational state. This has been demonstrated and used to study the $N_2(X^1\Sigma_g^+) - N_2(X^1\Sigma_g^+)$ system in the work of Macdonald *et al*. [11, 12] Multi-temperature models are constructed by assuming that all states are contained in the same group, but that the time scale of rotational and vibrational processes are different, resulting in a two-temperature distribution within each species. [13, 14, 15] The MGME-CGM has previously been applied to study both electronic atomic states as well as rovibrational states of diatomic molecules. [9, 10, 11, 12, 16, 17, 18, 19, 20, 21, 22, 23, 24]

Previous studies using the MGME-CGM method for the $N_2(X^1\Sigma_g^+) - N(^4S_u)$ system made use of kinetic data calculated by applying the appropriate weighting to StS data. [10] However, due to the limitations on calculating StS data, this was impossible for the $N_2(X^1\Sigma_g^+) - N_2(X^1\Sigma_g^+)$ system. Therefore, previous studies on $N_2(X^1\Sigma_g^+) - N_2(X^1\Sigma_g^+)$ relied on directly computing kinetic data for the MGME-CGM using the coarse-grain quasi-classical trajectory (CG-

QCT) method. [11, 12] This approach relied on the assumption that the internal temperature within each group was in thermal equilibrium with the translational mode, requiring only reaction rate coefficients to complete the model. However, this approach meant that to achieve good agreement with the direct molecular simulation (DMS) method[25, 26, 27, 28] required 60 groups. Relaxing this assumption in studies of the $N_2(X^1\Sigma_g^+) - N(^4S_u)$ system achieved good agreement with as few as 2-3 groups. Because the ultimate goal of this approach is application to CFD or DSMC, reducing the number of groups is paramount. The primary challenge with allowing the temperature to vary within the groups is the breakdown of the detailed balance condition among groups: we can no longer apply detailed balance at a group level. Therefore, to simulate recombination for example, we need to apply detailed balance at a microscopic level to tabulate recombination rates.

In this paper we propose an extended framework for coupling the coarse-grain model with scattering calculations to construct the full maximum entropy linear coarse-grain model for general molecule-molecule (*e.g.*, diatom-diatom) systems. The result is a general framework for obtaining grouped kinetic data for the coarse grain model called the Multi-Group Maximum-Entropy Quasi-Classical Trajectory (MGME-QCT) method. This extends upon previous work by the authors, [11, 12] by computing all kinetic data for the linear coarse grain model by sampling QCT and invoking detailed balance at a microscopic level. There are two key advantages to this approach: first, it allows for the calculation of recombination rates from dissociating trajectories, eliminating the need to run recombination trajectories, and second, it allows for the calculation of all the kinetic data for excitation type reactions from only trajectories in one direction (*e.g.*, only exothermic trajectories) ensuring the model is self-consistent. First, we present the general framework for calculating kinetic data for the grouping model from QCT calculations. Second, we present sample calculations of the grouped kinetic data with comparison against grouped known StS kinetic data for the $N_2(X^1\Sigma_g^+) - N(^4S_u)$ system.

## MULTI-GROUP MAXIMUM ENTROPY QUASI-CLASSICAL TRAJECTORY METHOD

The MGME-QCT method couples the MGMG-CGM with the QCT method to construct a reduced order model for kinetics without the calculation intensive step of pre-computing StS kinetic data for a system. The multi-group maximum entropy coarse grain model has previously been described in detail in Ref. [10]. This approach to model reduction can be summarized in two steps:

1. **Local representation and reconstruction:** energy states are lumped into groups containing states which share some properties (*e.g.*, similar energy, vibrational quantum number, *etc.*) and the distribution within the group is derived by maximizing the entropy within the group subject to some constraints.
2. **Macroscopic governing equations:** macroscopic governing equations are derived by taking moments of the master equation and making use of the distribution of states within each group derived in step 1.

This work will make use of the maximum entropy "linear" coarse grain model (MEL-CGM). In this approach, states within the same group are assumed to equilibrate quickly, resulting in an equilibrium Boltzmann distribution within each group. However, equilibrium is not assumed among all groups, and the temperature within each group varies. In this work we will focus on the $N_2(X^1\Sigma_g^+) - N(^4S_u)$ system because it has known state-to-state kinetics and can be used to verify this approach to computing kinetic data. Therefore, the nitrogen molecules are grouped according to the MEL-CGM. The distribution of states within each group is denoted by $\mathcal{F}^i_{N_2(p)}$ within group $p$ of species $N_2$ molecules and is given by:

$$\mathcal{F}^i_{N_2(p)}(T^p_{N_2}) = \frac{n^i_{N_2}}{n^p_{N_2}} = \frac{{}^0Q^i_{N_2}(T^p_{N_2})}{{}^0Q^p_{N_2}(T^p_{N_2})} \tag{1}$$

where $T^p_{N_2}$ gives the group internal temperature, $n^i_{N_2}$ and $n^p_{N_2}$ denote respectively the number density of state $i$ and group $p$ of $N_2$. The state and group partition functions are denoted by ${}^0Q^i_{N_2}(T^p_{N_2})$ and ${}^0Q^p_{N_2}(T^p_{N_2})$ respectively:

$${}^mQ^i_{N_2}(T^p_{N_2}) = g^i_{N_2}\left(E^i_{N_2}\right)^m \exp\left(-\frac{E^i_{N_2}}{k_B T^p_{N_2}}\right), \quad {}^mQ^p_{N_2}(T^p_{N_2}) = \sum_{i\in\mathcal{I}_p} {}^mQ^i_{N_2}(T^p_{N_2}) \tag{2}$$

where set $\mathcal{I}_p$ contains the states in group $p$, $g^i_{N_2}$ and $E^i_{N_2}$ denote respectively the degeneracy and energy of state $i$, $k_B$ denotes the Boltzmann constant, and $m$ denotes the order of the moment for the partition function which will be

used later when writing the conservation equations for the groups. This is derived by maximizing the entropy within a group subject to constraints on the group mass and energy:

$$n^p_{\mathrm{N}_2} = \sum_{i \in \mathcal{I}_p} n^i_{\mathrm{N}_2}, \quad e^p_{\mathrm{N}_2} = \sum_{i \in \mathcal{I}_p} n^i_{\mathrm{N}_2} E^i_{\mathrm{N}_2} \tag{3}$$

where $e^p_{\mathrm{N}_2}$ denotes the energy density of group $p$. This work is not concerned with the manner in which states are grouped and will make use of a simple energy based grouping scheme in which states close in energy are lumped together. Details on the influence of grouping strategy on the results can be found in Refs. [11, 12], and details on advanced grouping strategies can be found in Ref. [24].

In this work, we consider the interaction between atomic and molecular nitrogen with internal states of the molecules (*e.g.*, rovibrational) denoted by global indices $(i, j)$. The interaction between the atom and molecule can result in excitation or dissociation processes:

$$\mathrm{N}_2(i) + \mathrm{N} \underset{\kappa^{\mathrm{E}}_{j,i}}{\overset{\kappa^{\mathrm{E}}_{i,j}}{\rightleftharpoons}} \mathrm{N}_2(j) + \mathrm{N}$$

$$\mathrm{N}_2(i) + \mathrm{N} \underset{\kappa^{\mathrm{R}}_{i}}{\overset{\kappa^{\mathrm{D}}_{i}}{\rightleftharpoons}} 3\mathrm{N}$$

The reaction rates for these interactions are denoted by $\kappa^{\mathrm{E}}_{i,j}$, $\kappa^{\mathrm{E}}_{j,i}$, $\kappa^{\mathrm{D}}_{i}$, and $\kappa^{\mathrm{R}}_{i}$ for excitation, de-excitation, dissociation, and recombination respectively, and are a function of the translational temperature, $T$. The conservation equations are derived by taking moments (denoted by $m$) of the master equation and making use of the reconstruction function in Eq. (1). The group governing equations for the molecules comprise group mass conservation and group energy conservation:

$$\frac{dn^p_{\mathrm{N}_2}}{dt} = \sum_{\substack{q \in \mathcal{I} \\ q \neq p}} \left( -{}^0K_{p,q} n^p_{\mathrm{N}_2} n_{\mathrm{N}} + {}^0\bar{K}_{p,q} n^q_{\mathrm{N}_2} n_{\mathrm{N}} \right) + \left( -{}^0C_p n^p_{\mathrm{N}_2} n_{\mathrm{N}} + {}^0\bar{C}_p n^3_{\mathrm{N}} \right), \quad p \in \mathcal{I}, \tag{4}$$

$$\frac{de^p_{\mathrm{N}_2}}{dt} = \sum_{q \in \mathcal{I}} \left( -{}^1K_{p,q} e^p_{\mathrm{N}_2} n_{\mathrm{N}} + {}^1\bar{K}_{p,q} e^q_{\mathrm{N}_2} n_{\mathrm{N}} \right) + \left( -{}^1C_p e^p_{\mathrm{N}_2} n_{\mathrm{N}} + {}^1\bar{C}_p n^3_{\mathrm{N}} \right), \quad p \in \mathcal{I}, \tag{5}$$

Where ${}^0K_{p,q}$ and ${}^1K_{p,q}$ (${}^0\bar{K}_{p,q}$ and ${}^1\bar{K}_{p,q}$) denote respectively the depleting (replenishing) reaction rates and energy transfer coefficients due to excitation processes, ${}^0C_p$ and ${}^1C_p$ (${}^0\bar{C}_p$ and ${}^1\bar{C}_p$) denote respectively the dissociation (recombination) reaction rates and energy transfer coefficients, and the set $\mathcal{I}$ denotes the set of all groups. The conservation of mass equations, Eq. 4, considers only excitation reactions among groups, hence the summation is taken only over groups different from $p$. However, it is important to note that excitation reactions within a group can change the energy of that group. Therefore, in the conservation of group energy equations, Eq. 5, we consider excitation from group $p$ to all possible final groups, including group $p$. In addition, the dissociation and recombination reactions only pertain to a single group, and each rate or energy transfer coefficient only shows up in the respective group equations. Conservation equations can be written in this manner for each species considered in the MEL-CGM model (*e.g.*, $\mathrm{N}_2(\mathrm{X}^1\Sigma^+_{\mathrm{g}})$ in this work).

The reaction rates and energy transfer coefficients from Eqs. (4) and (5) (${}^mK_{p,q}$, ${}^m\bar{K}_{p,q}$, ${}^mC_p$, ${}^m\bar{C}_p$) are weighted

averages of the microscopic reaction rates ($\kappa^{\mathrm{E}}_{i,j}$, $\kappa^{\mathrm{E}}_{j,i}$, $\kappa^{\mathrm{D}}_{i}$, $\kappa^{\mathrm{R}}_{i}$).

$$ {}^{m}K_{p,q} = \frac{{}^{0}Q^{p}_{\mathrm{N}_2}(T^{p}_{\mathrm{N}_2})}{{}^{m}Q^{p}_{\mathrm{N}_2}(T^{p}_{\mathrm{N}_2})} \sum_{i\in\mathcal{I}_p}\sum_{j\in\mathcal{I}_q} \kappa^{\mathrm{E}}_{i-j}(E_i)^m \left[\frac{g_i \exp\left(-\frac{E_i}{k_B T^{p}_{\mathrm{N}_2}}\right)}{{}^{0}Q^{p}_{\mathrm{N}_2}(T^{p}_{\mathrm{N}_2})}\right] \tag{6} $$

$$ {}^{m}\bar{K}_{p,q} = \frac{{}^{0}Q^{q}_{\mathrm{N}_2}(T^{q}_{\mathrm{N}_2})}{{}^{0}Q^{q}_{\mathrm{N}_2}(T^{q}_{\mathrm{N}_2})} \sum_{i\in\mathcal{I}_p}\sum_{j\in\mathcal{I}_q} \kappa^{\mathrm{E}}_{j-i}(E_i)^m \left[\frac{g_j \exp\left(-\frac{E_j}{k_B T^{q}_{\mathrm{N}_2}}\right)}{{}^{0}Q^{q}_{\mathrm{N}_2}(T^{q}_{\mathrm{N}_2})}\right] \tag{7} $$

$$ {}^{m}C_{p} = \frac{{}^{0}Q^{p}_{\mathrm{N}_2}(T^{p}_{\mathrm{N}_2})}{{}^{m}Q^{p}_{\mathrm{N}_2}(T^{p}_{\mathrm{N}_2})} \sum_{i\in\mathcal{I}_p} \kappa^{\mathrm{D}}_{i}(E_i)^m \left[\frac{g_i \exp\left(-\frac{E_i}{k_B T^{p}_{\mathrm{N}_2}}\right)}{{}^{0}Q^{p}_{\mathrm{N}_2}(T^{p}_{\mathrm{N}_2})}\right] \tag{8} $$

$$ {}^{m}\bar{C}_{p} = \sum_{i\in\mathcal{I}_p} \kappa^{\mathrm{R}}_{i}(E_i)^m \tag{9} $$

The forward group rates, ${}^{m}K_{p,q}$ and ${}^{m}C_{p}$, can be obtained by sampling the initial states for scattering trajectories from the distributions given by $\mathcal{F}^{i}_{A(p)}(T^{p}_{A})$. This process is detailed in Ref. [11]. This approach poses a problem for obtaining reverse reaction rates and energy transfer coefficients for two reasons: (1) it is impractical to obtain recombination rates through QCT when we have dissociation data and (2) to construct a self consistent model, we would like a relationship between forward and reverse reaction rates and energy transfer coefficients. Because the group rates and energy transfer coefficients are in general a function of two parameters ($T$ and $T^{p}_{\mathrm{N}_2}$), a detailed balance relationship does not hold at a group level. Therefore, by invoking detailed balance on a microscopic level, we can obtain expressions for the reverse reaction rates and energy transfer coefficients (${}^{m}\bar{K}_{p,q}$ and ${}^{m}\bar{C}_{p}$) based on the forward microscopic rates ($\kappa^{\mathrm{E}}_{i,j}$ and $\kappa^{\mathrm{D}}_{i}$):

$$ {}^{m}\bar{K}_{p,q} = \frac{{}^{0}Q^{p}_{\mathrm{N}_2}(T)}{{}^{m}Q^{q}_{\mathrm{N}_2}(T^{q}_{\mathrm{N}_2})} \sum_{i\in\mathcal{I}_p}\sum_{j\in\mathcal{I}_q} \kappa^{\mathrm{E}}_{i-j}(E_i)^m \left[\frac{g_i \exp\left(-\frac{E_i}{k_B T}\right)}{{}^{0}Q^{p}_{\mathrm{N}_2}(T)}\right] \left[\frac{\exp\left(-\frac{E_j}{k_B T^{q}_{\mathrm{N}_2}}\right)}{\exp\left(-\frac{E_j}{k_B T}\right)}\right] \tag{10} $$

$$ {}^{m}\bar{C}_{p} = \frac{{}^{0}Q^{p}_{\mathrm{N}_2}(T)Q^{\mathrm{trans}}_{\mathrm{N}_2}(T)}{\left(Q^{\mathrm{int}}_{\mathrm{N}}(T)Q^{\mathrm{trans}}_{\mathrm{N}}(T)\right)^2} \sum_{i\in\mathcal{I}_p} \kappa^{\mathrm{D}}_{i}(E_i)^m \left[\frac{g_i \exp\left(-\frac{E_i}{k_B T}\right)}{{}^{0}Q^{p}_{\mathrm{N}_2}(T)}\right] \tag{11} $$

where $Q^{trans}_{S}(T)$ denotes the translational partition function for species $S$ at temperature $T$:

$$ Q^{trans}_{S}(T) = \left(\frac{2\pi m_S k_B T}{h^2_P}\right)^{3/2} \tag{12} $$

where $m_S$ denotes the particle mass of species $S$ and $h_P$ denotes Planck's constant. The advantage is that now Eqs. (10) and (11) are written in terms of forward rates at the translational temperature with a scaling factor on the final state which can be applied in post-processing the trajectories. This ensures that detailed balance will hold and the system will proceed to equilibrium given enough time, and eliminates the need to run recombination trajectories, overcoming both of the problems described earlier. Equations (6), (8), (10), and (11) comprise the expressions used to obtain grouped kinetic data in the MEL-CGM. The averaging over the initial states is done by sampling the initial states at the prescribed temperature (*e.g*, for Eq. (6) at $T^{p}_{\mathrm{N}_2}$, or for Eq. (10) at $T$). Everything else can be obtained as a post-processing step after many trajectories have been calculated (*e.g.*, the summation over the final states). Further details on the QCT process and sampling approach to the initial states can be found in Refs. [29, 30, 31, 11].

In addition to constructing the full MEL-CGM through QCT calculations, we can quantify the error due to sampling through the relationship:

$$ \mathrm{var}(x) = \langle x^2 \rangle - \langle x \rangle^2 \tag{13} $$

Where $x$ is the quantity of interest (*e.g.*, reaction rate, energy transfer coefficient, etc.), and the $\langle x \rangle$ denotes the mean value of $x$. In the results, error bars for the rates and energy transfer coefficients will denote one standard deviation, $s = \sqrt{\mathrm{var}(x)}$.

## GROUPED KINETIC DATA

In this work, we are focused on validating the MGME-QCT method using the $N_2(X^1\Sigma_g^+) - N(^4S_u)$ system which has known state-to-state (StS) kinetics. Therefore, we will compare the kinetic data obtained using the MGME-QCT method with the StS data grouped in the same manner. The StS data for excitation processes comprises only data which results from exothermic trajectories due to the increased accuracy of this data. Further details on the StS kinetic data can be found in Ref. [3]. The MGME-QCT data is available for both exothermic and endothermic data for the excitation data because the QCT trajectories occur in both directions. Therefore, two kinetic mechanisms for excitation can be constructed by using either only exothermic or only endothermic data. This will be done for comparison. The results will make use of a simple energy based grouping scheme using either 60 or 6 groups, denoted by MEL(60) and MEL(6) respectively. The trajectory data was calculated for the MEL(60) model using 192,000 trajectories from each initial group ($p$) at translational temperature $T = 10\,000$ K and group internal temperatures of $T^p_{N_2} = (2000\,\text{K}, 5000\,\text{K}, 10\,000\,\text{K})$. The kinetic data for the MEL(6) model was retrieved by re-grouping the kinetic data for the MEL(60) model with the appropriate weighting.

Figure 1 shows the forward energy transfer coefficients for the excitation reaction for the MEL(6) model from a fixed initial group ($q = 2$). The rates computed from exothermic trajectories are in excellent agreement with the rates computed from the StS data. Moreover, the statistical error associated with the exothermic rate data is generally very low (the mean error for all energy transfer coefficients computed using exothermic trajectory data is 1.5%). The rate data computed using endothermic trajectories is in very good agreement with the grouped StS data as well. However, the higher energy jumps exhibit higher error (the mean error for all energy transfer coefficients computed using endothermic trajectory data is 14.1%).

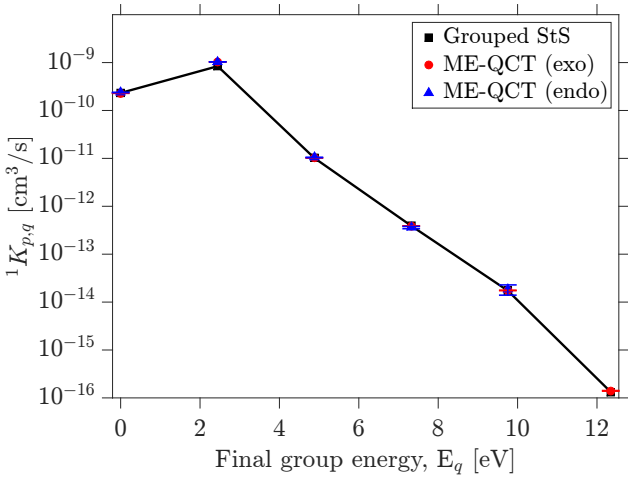


**FIGURE 1.** Grouped energy transfer coefficients for excitation reaction MEL(6), $N_2(p = 2) + N \rightleftharpoons N_2(q) + N$ ($^1K_{p-q}$) at T = 10 000 K and $T^p_{N_2} = 5000$ K; error bars denote one standard deviation.

Figure 2 shows the dissociation and recombination energy transfer rates for the MEL(60) model. Similar to what was observed for the excitation reaction, the energy transfer coefficients for high energy jumps (*e.g.*, dissociation from groups below around 4 eV) exhibit high statistical error. Despite this fact, Fig. 2 highlights the key advantage to this framework: reaction rates and energy transfer coefficients for the recombination process can be computed. Because the recombination rates are obtained from dissociating trajectories through detailed balance, there are two key advantages: first, this ensures that detailed balance is obeyed, ensuring that the system will reach equilibrium given enough time; second, recombination rates and energy transfer coefficients can be obtained from dissociating trajectories, eliminating the need to run recombination trajectories. Because the recombination energy transfer coefficients are obtained from dissociation trajectories, the error of the recombination rates mirrors that observed for the dissociation rates.

Figure 3 shows the variation of the excitation forward energy transfer coefficient for the MEL(6) model from group 2 to group 3 with the group internal and translational temperatures. This was computed by grouping the StS data to enable calculation at many internal temperatures. The variation of the rate with translational temperature is

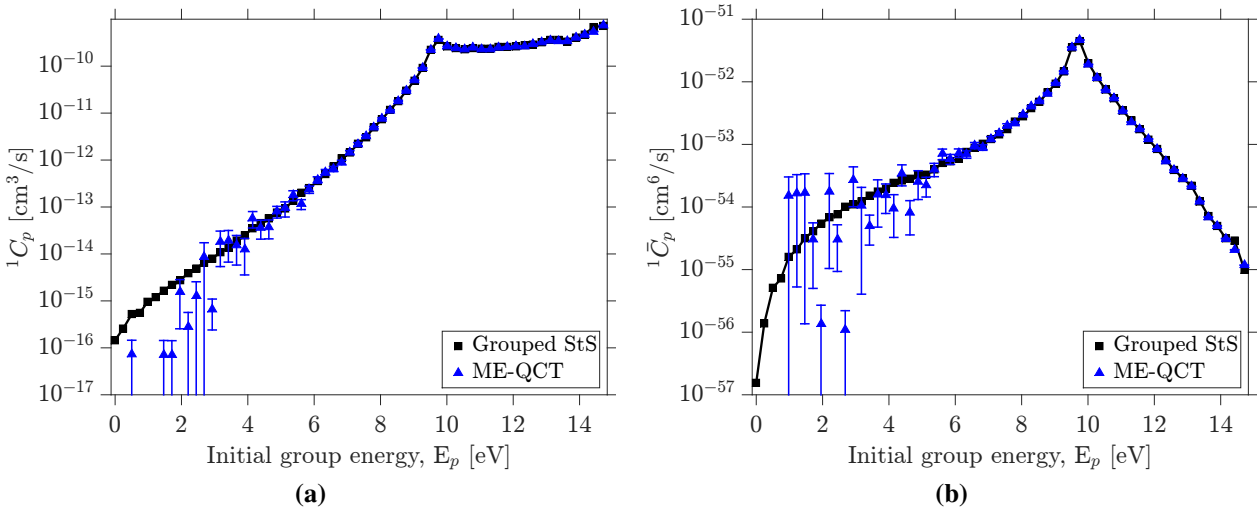


**FIGURE 2.** Grouped energy transfer coefficients for dissociation reaction for MEL(60) from group $q$, $N_2(q) + N \rightleftharpoons 3N$ at T = 10 000 K and $T^p_{N_2}$ = 5000 K; error bars denote one standard deviation: **(a)** $C_p$, **(b)** $\bar{C}_p$.

quite strong, as expected. However, the internal temperature also has a significant impact on the rates, particularly at high translational temperatures. The inset shows the variation of the coefficient due to internal temperature at $T$ = 10 000 K from the MGME-QCT models and the grouped StS as well as the variation at $T$ = 20 000 K from the grouped StS data. This demonstrates the importance of calculating kinetic data at various internal and translational temperatures, as the impact of both parameters on the kinetic data is significant.

## CONCLUSIONS

In this paper, a general model reduction framework for studying non-equilibrium dissociation and energy transfer has been presented. In this approach, the multi-group maximum-entropy linear coarse-grain model is coupled with quasi-classical trajectory calculations to directly obtain the complete set of kinetic data for the multi-group maximum-entropy linear coarse-grain model. We apply detailed balance at a microscopic to ensure a self consistent model which will proceed to equilibrium given enough time. Moreover, this allows the coarse grain model to be constructed using the exothermic trajectory data which are characterized by lower statistical error. Finally, the MGME-QCT model is compared to the grouped StS kinetic data for the $N_2(X^1\Sigma^+_g) - N(^4S_u)$ system for validation, with excellent agreement.

## ACKNOWLEDGMENTS

Ms. R. Macdonald was supported by the Department of Defense (DoD) through the National Defense Science & Engineering Graduate Fellowship (NDSEG) Program. Dr. M. Panesi was supported by the Air Force Office of Scientific Research Young Investigators Program FA9550-15-1-0132 with Program Officer Dr. Ivett Leyva. The views and conclusions contained herein are those of the authors and should not be interpreted as necessarily representing the official policies or endorsements, either expressed or implied, of the AFOSR or the US government.

## REFERENCES

[1] R. L. Jaffe, D. W. Schwenke, G. Chaban, and W. Huo, "Vibrational and rotational excitation and relaxation of nitrogen from accurate theoretical calculations," AIAA Paper 2008–1208 (2008) 46th AIAA Aerospace Sciences Meeting and Exhibit, Reno, NV.

[2] G. Chaban, R. L. Jaffe, D. W. Schwenke, and W. Huo, "Dissociation cross-sections and rate coefficients for nitrogen from acccurate theoretical calculations," AIAA Paper 2008–1209 (2008) 46th AIAA Aerospace Sciences Meeting and Exhibit, Reno, NV.

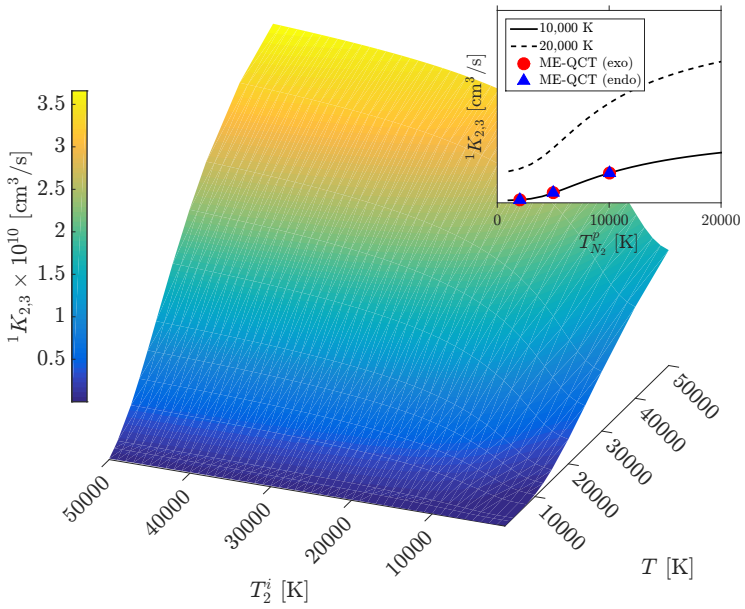


**FIGURE 3.** Excitation energy transfer coefficients for MEL(6) from group 2 to group 3 at varying translational and group internal temperature. Inset: variation of energy transfer coefficient on bin internal temperature at 10 000 K for grouped StS (solid line), exothermic MGME-QCT (circles), and endothermic MGME-QCT (triangles) and at 20 000 K for grouped StS (broken line).


[3] M. Panesi, R. L. Jaffe, D. W. Schwenke, and T. E. Magin, J. Chem. Phys **138**, p. 044312 (2013).
[4] J. G. Kim and I. D. Boyd, Chem. Phys. **415**, 237–246 (2013).
[5] R. L. Macdonald, A. Munafò, C. O. Johnston, and M. Panesi, Phys. Rev. Fluids **1**, p. 043401Aug (2016).
[6] F. Esposito, E. Garcia, and A. Laganà, Plasma Sources Science and Technology **26**, p. 045005 (2017).
[7] R. D. Levine and R. B. Bernstein, *Molecular Reaction Dynamics and Chemical Reactivity* (Oxford University Press, 1987).
[8] M. Kulakhmetov, M. Gallis, and A. Alexeenko, The Journal of Chemical Physics **144**, p. 174302 (2016), https://doi.org/10.1063/1.4947590 .
[9] M. Panesi, T. E. Magin, A. Bourdon, A. Bultel, and O. Chazot, J. Thermophys. Heat Transfer **25**, 361–374 (2011).
[10] Y. Liu, M. Panesi, A. Sahai, and M. Vinokur, J. Chem. Phys. **142**, p. 134109 (2015).
[11] R. L. Macdonald, R. L. Jaffe, D. W. Schwenke, and M. Panesi, The Journal of Chemical Physics **148**, p. 054309 (2018), https://doi.org/10.1063/1.5011331 .
[12] R. L. Macdonald, M. S. Grover, T. E. Schwartzentruber, and M. Panesi, The Journal of Chemical Physics **148**, p. 054310 (2018), https://doi.org/10.1063/1.5011332 .
[13] C. Park, J. Thermophys. Heat Transfer **3**, 233–244 (1989).
[14] C. Park, J. Thermophys. Heat Transfer **7**, 385–398 (1993).
[15] C. Park, J. T. Howe, R. L. Jaffe, and G. V. Candler, J. Thermophys. Heat Transfer **8**, 9–23 (1994).
[16] A. Munafò, M. Panesi, R. L. Jaffe, G. Colonna, A. Bourdon, and T. E. Magin, Eur. Phys. Jour. D **66**, p. 188 (2012).
[17] H. P. Le, A. P. Karagozian, and J.-L. Cambier, Phys. Plasmas **20**, p. 123304 (2013).
[18] C. O. Johnston and M. Panesi, Phys. Rev. Fluids **3**, p. 013402Jan (2018).
[19] M. Panesi and A. Lani, Phys. Fluids **25**, p. 057101 (2013).
[20] A. Munafò, M. Panesi, and T. E. Magin, Phys. Rev. E **89**, p. 023001 (2014).
[21] A. Munafò and T. E. Magin, Phys. Fluids **26**, p. 097102 (2014).
[22] A. Munafò, Y. Liu, and M. Panesi, Physics of Fluids **27**, p. 127101 (2015).
[23] A. Munafò, N. N. Mansour, and M. Panesi, Astrophys. J. **838**, p. 126 (2017).
[24] A. Sahai, B. Lopez, C. O. Johnston, and M. Panesi, The Journal of Chemical Physics **147**, p. 054107 (2017), http://dx.doi.org/10.1063/1.4996654 .

[25] P. Norman, P. Valentini, and T. Schwartzentruber, Journal of Computational Physics **247**, 153 – 167 (2013).
[26] P. Valentini, T. E. Schwartzentruber, J. D. Bender, I. Nompelis, and G. V. Candler, Physics of Fluids **27** (2015).
[27] P. Valentini, T. E. Schwartzentruber, J. D. Bender, and G. V. Candler, Phys. Rev. Fluids **1**, p. 043402Aug (2016).
[28] T. E. Schwartzentruber, M. S. Grover, and P. Valentini, J. Thermophys. Heat Transfer **0**, 1–12 (2017).
[29] M. Karplus, R. N. Porter, and R. D. Sharma, The Journal of Chemical Physics **43**, 3259–3287 (1965).
[30] D. W. Schwenke, J. Chem. Phys. **89**, 2076–2091 (1988).
[31] R. L. Jaffe, D. W. Schwenke, and M. Panesi, in *Hypersonic Nonequilibrium Flows: Fundamentals and Recent Advances*, edited by E. Josyula (American Institute of Aeronautics and Astronautics, 2015) Chap. 3,, pp. 103–158.